Pergamon

Int. J. Solids Structures Vol. 31, No. 24, pp. 3443–3455, 1994

0020-7683/94 $7.00 + .00

0020-7683(94)00086-7

CRACK DEFLECTION AT AN INTERFACE BETWEEN DISSIMILAR ELASTIC MATERIALS: ROLE OF RESIDUAL STRESSES

MING YUAN HE and ANTHONY G. EVANS

Materials Department, College of Engineering, University of California, Santa Barbara, CA 93106-5050, U.S.A.

and

JOHN W. HUTCHINSON

Division of Applied Sciences, Harvard University, Cambridge, MA 02138, U.S.A

(*Received* 19 *October* 1993; *in revised form* 20 *April* 1994)

Abstract—A crack intersecting an interface between two dissimilar materials may advance by either penetrating through the interface or deflecting into the interface. The competition between deflection and penetration can be assessed by comparison of *two ratios*: (i) the ratio of the energy release rates for interface cracking and crack penetration; and (ii) the ratio of interface to material fracture energies. Residual stresses caused by thermal expansion misfit can influence the energy release rates of both the deflected and penetrating crack. This paper analyses the role of residual stresses. The results reveal that expansion misfit can be profoundly important in systems with planar interfaces (such as layered materials, thin film structures, etc.), but generally can be expected to be of little significance in fiber composites. This paper corrects an earlier result for the ratio of the energy release rate for the doubly deflected crack to that for the penetrating crack in the absence of residual stress.

1. INTRODUCTION

In an earlier paper [He and Hutchinson (1989b), hereafter designated by HH], a study was made of the tendency of a crack meeting a bimaterial interface to either deflect into the interface or penetrate through the interface into the next layer. The analysis was conducted in terms of the relative energy release ratio for the crack deflecting into the interface $\mathcal{G}_d$ and for the crack penetrating the interface $\mathcal{G}_p$. The competition between interface cracking and substrate cracking was then designated to depend on whether $\mathcal{G}_d/\mathcal{G}_p$ was either greater or less than the ratio of the fracture energy of the interface Γ_i and that of the adjoining layer, Γ_s. The analysis in HH is asymptotic and the predictions are accurate whenever the length of the branch crack emanating from the main crack tip is very small compared with all other lengths in the problem, including the length of the main crack itself. These results combined with the basic mechanics of interfacial cracks (He and Hutchinson, 1989a) have been used to define the role of debonding in fiber-reinforced, brittle matrix composites (Evans *et al.*, 1989a,b), as well as interface decohesion in layered materials and laminates. However, the analysis in HH neglected residual stresses which may be important in some cases. In the presence of residual stresses, σ_t and σ_n (Fig. 1), it will be shown that two additional nondimensional length parameters become important

$$\eta_n = \frac{\sigma_n a_d^{\lambda}}{k_I}, \quad \eta_t = \frac{\sigma_t a_p^{\lambda}}{k_I} \tag{1}$$

where a is the length of the branch crack either at the interface, a_d, or in the next layer, a_p, λ is the stress singularity exponent for the main crack (defined below) and k_I is a factor proportional to the applied far field. The role of these parameters in the competition between interface cracking and substrate cracking is the subject of this paper.

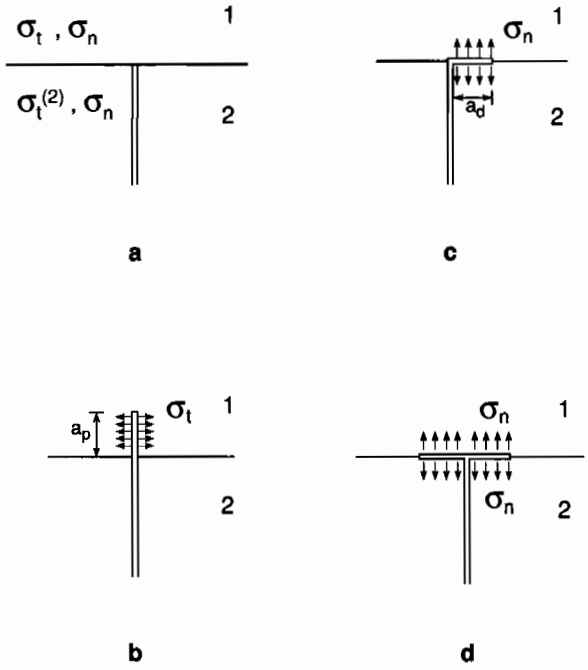

Fig. 1. Crack geometries used in this analysis.

Two isotropic, elastic materials bonded at the interface and containing plane strain cracks are considered (Fig. 1). The two elastic mismatch parameters governing plane strain problems are

$$\alpha = (\bar{E}_1 - \bar{E}_2)/(\bar{E}_1 + \bar{E}_2) \tag{2}$$

$$\beta = \tfrac{1}{2}(\mu_1(1-2\nu_2) - \mu_2(1-2\nu_1))/(\mu_1(1-\nu_2) + \mu_2(1-\nu_1)) \tag{3}$$

where E, μ and ν denote Young's modulus, shear modulus and Poisson's ratio, respectively, and $\bar{E} = E/(1-\nu^2)$. An "oscillation index" ε that depends on β is defined as,

$$\varepsilon = \frac{1}{2\pi} \ln\left(\frac{1-\beta}{1+\beta}\right). \tag{4}$$

2. STRESS INTENSITY FACTORS AND ENERGY RELEASE RATES

The main crack is considered to be semi-infinite and perpendicular to the interface, with its tip at the interface. Symmetric loading with respect to the crack plane is applied and the stress σ_{xx} in the material ahead of the crack (designated material 1) is characterized by

$$\sigma_{xx}(0, y) = k_1(2\pi y)^{-\lambda} \tag{5}$$

where λ is real and depends on α and β according to (Zak and William, 1963)

$$\cos \lambda\pi = \frac{2(\beta-\alpha)}{1+\beta}(1-\lambda)^2 + \frac{\alpha+\beta^2}{1-\beta^2} \tag{6}$$

and k_1 is a stress intensity-like factor related to the applied loads. Knowledge of k_1 requires solution of the problem of the main crack on the tip at the interface with prescribed geometry and loading. Our discussion will not require this knowledge. Values of λ are given

Table 1. The variables $\lambda, c, h, d_R, d_I, g_R, g_I$ (singly deflected crack) as a function of α

α	λ	c	h	d_R	d_I	g_R	g_I
−0.9	0.8175	0.6104	1.314	0.0272	−0.6212	1.493	0.0229
−0.8	0.7450	0.6877	1.358	0.0613	−0.6281	1.546	0.0468
−0.7	0.6920	0.7493	1.395	0.1023	−0.5805	1.587	0.0692
−0.6	0.6495	0.7830	1.428	0.1464	−0.5389	1.622	0.0905
−0.5	0.6142	0.8224	1.458	0.1877	−0.5005	1.657	0.1110
−0.4	0.5843	0.8595	1.487	0.2283	−0.4630	1.680	0.1307
−0.3	0.5586	0.8953	1.515	0.2669	−0.4313	1.706	0.1490
−0.2	0.5364	0.9301	1.543	0.3043	−0.4017	1.727	0.1669
−0.1	0.5170	0.9647	1.571	0.3381	−0.3741	1.746	0.1835
0.0	0.5000	0.9990	1.599	0.3707	−0.3490	1.763	0.1993
0.1	0.4850	1.034	1.628	0.4011	−0.3259	1.778	0.2151
0.2	0.4718	1.069	1.657	0.4292	−0.3044	1.790	0.2296
0.3	0.4601	1.104	1.689	0.4553	−0.2842	1.802	0.2444
0.4	0.4496	1.142	1.722	0.4823	−0.2662	1.820	0.2575
0.5	0.4402	1.181	1.757	0.5019	−0.2492	1.831	0.2712
0.6	0.4318	1.222	1.795	0.5226	−0.2327	1.841	0.2841
0.7	0.4242	1.267	1.836	0.5419	−0.2177	1.849	0.2952
0.8	0.4173	1.315	1.881	0.5601	−0.2041	1.857	0.3078
0.9	0.4111	1.368	1.931	0.5761	−0.1903	1.867	0.3188

as functions of α for $\beta = 0$ in Table 1. The main crack is imagined to advance in one of the three ways indicated in Fig. 1: either penetration through the interface [Fig. 1(b)] or deflection into the interface, occurring either as a single kink [Fig. 1(c)] or a double kink [Fig. 1(d)]. As in HH, it will be assumed that the putative length of the branch crack (a_p or a_d) is very small compared with all other geometric length quantities and, in particular, small compared with the length of the main crack.

In the case of penetration, the stress state at the advancing tip is model I. By dimensional considerations, the stress intensity factors must depend on k_I, a_p and the residual stress parallel to the interface,† σ_t, in accordance with

$$K_I = c(\alpha)k_I a_p^{1/2-\lambda} + h(\alpha)\sigma_t a_p^{1/2} \tag{7}$$

where c and h are dimensionless functions of α and β. To reduce the number of parameters in presenting the results, we will *emphasize* the role of α and take $\beta = 0$. Experience with related problems suggest that of the two parameters, the dependence on α is the stronger one. The residual stress component σ_n has no effect on K_I, since it acts parallel to the advancing crack. The energy release rate is

$$\mathcal{G}_p \equiv \frac{1-\nu_1}{2\mu_1} K_I^2$$

$$= \frac{1-\nu_1}{2\mu_1} [c^2 k_I^2 a_p^{1-2\lambda} + 2chk_I\sigma_t a_p^{1-\lambda} + h^2\sigma_t^2 a_p]. \tag{8}$$

For deflected cracks, the stress on the interface directly ahead of the right-hand tip [either (c) or (d) in Fig. 1] is characterized by (Rice, 1988)

$$\sigma_{yy}(x,0) + i\sigma_{xy}(x,0) = (K_1 + iK_2)(2\pi r)^{-1/2} r^{i\varepsilon} \tag{9}$$

where $r = x - a$. When $\beta = 0$, K_1 and K_2 can be regarded as conventional mode I and mode II stress intensity factors, so that

† The residual stresses in the material containing the main crack (material 2) can be included in the applied loads for the main crack and therefore are contained in k_I.

$$\sigma_{yy} = K_1(2\pi r)^{-1/2}, \quad \sigma_{xy} = K_2(2\pi r)^{-1/2}. \tag{10}$$

By dimensional considerations analogous to those given in HH, K_1 and K_2 must depend on k_1, a and the in-plane residual stress perpendicular to the interface σ_n according to

$$K_1 + iK_2 = k_1 a_d^{1/2-\lambda} d(\alpha) + \sigma_n a_d^{1/2} g(\alpha) \tag{11}$$

where $d = d_R + id_I$ and $g = g_R + ig_I$ are dimensionless complex functions of α. Here again, it has been assumed that $\beta = 0$. The stress component σ_t has no effect on K_1 and K_2, since it acts parallel to the advancing crack.

The energy release rate at the tip of the deflected crack is then

$$\mathcal{G}_d = \frac{1}{\bar{E}_*}\{k_1^2 a_d^{1-2\lambda} |d|^2 + k_1\sigma_n a_d^{(1-\lambda)}(d\bar{g} + \bar{d}g) + |g|^2\sigma_n^2 a_d\} \tag{12}$$

where $(^-)$ denotes the complex conjugate and $\bar{E}_*$ is given by

$$\frac{1}{\bar{E}_*} = \left[\frac{1}{\bar{E}_1} + \frac{1}{\bar{E}_2}\right]\frac{1}{2}(1-\beta^2)$$

$$\equiv \frac{1-\beta^2}{(1-\alpha)\bar{E}_1}. \tag{13}$$

The ratio $\mathcal{G}_d/\mathcal{G}_p$ is thus

$$\frac{\mathcal{G}_d}{\mathcal{G}_p} = \frac{|d|^2 + \eta_n(d\bar{g} + \bar{d}g) + \eta_n^2|g|^2}{[c^2 + 2\eta_t ch + \eta_t^2 h^2](1-\alpha)}\left(\frac{a_d}{a_p}\right)^{1-2\lambda} \tag{14}$$

and depends only on the nondimensional parameters α, η_t, η_n and a_d/a_p.

Note that the phase angle Ψ of the stress intensity factors, which provides a measure of relative amount of mode II to mode I of the loading on the branched *interface crack*, is given by

$$\Psi \equiv \tan^{-1}\left(\frac{K_2}{K_1}\right) \tag{15}$$

which, with eqn (11), becomes,

$$\Psi \equiv \tan^{-1}\left(\frac{(d_I + g_I\eta_n)}{(d_R + g_R\eta_n)}\right). \tag{16}$$

The present results were obtained by allowing the "loading on the crack" to be that associated with σ_t and σ_n. All numbered results presented for the coefficients in the tables in this paper were computed using a finite element method with a refined mesh described in the Appendix. Many of the results were checked using the integral equation formulation

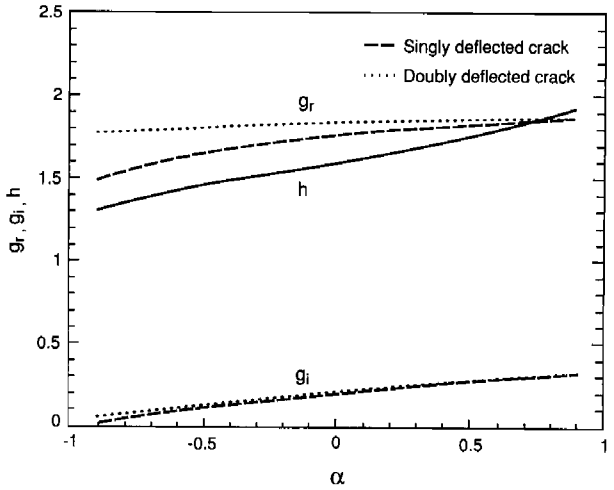

Fig. 2. Curves of h, g_R and g_I as a function of α.

of HH. It is found that g_I and g_R are relatively insensitive to α (Fig. 2), as tabulated in Table 1 for a singly deflected crack. The counterparts for doubly deflected cracks are given in Table 2. All results are for $\beta = 0$.

The ratio $\mathcal{G}_d/\mathcal{G}_p$ for $a_p = a_d$ is plotted in Fig. 3(a) as functions of α and η_t, for $\eta_n = 0$, where $\mathcal{G}_d$ is for the singly deflected crack. It is apparent that the residual stress σ_t begins to have a significant effect on this energy ratio when $|\eta_t| \gtrsim 0.1$. The ratio $\mathcal{G}_d/\mathcal{G}_p$ diminishes as the parameter η_t increases. Corresponding plots for $\eta_n = -0.1$ and $+0.1$ are shown in Figs 3(b) and 3(c). An equivalent set of plots for $\eta_t = 0$, 0.1 and -0.1, showing the influence of η_n, are summarized in Fig. 4, while the trends in the phase angle of the interface crack, as η_n varies, are given in Fig. 5. As would be expected, the ratio $\mathcal{G}_d/\mathcal{G}_p$ increases as the parameter η_n increases, reflecting the strong influence of residual stress normal to the interface as it changes from positive to negative.

A full set of computations has been carried out for the doubly deflected crack and it has been established that $\mathcal{G}_d/\mathcal{G}_p$ and Ψ depend on the stress parameters η_t and η_n in almost the same way as for the singly deflected crack (compare Tables 1 and 2). The small differences do not warrant presentation of a separate set of figures for this case. However, because an earlier paper by two of the present authors (He and Hutchinson, 1989b) contained incorrect results for the doubly deflected crack problem, we show in Figs 6(a)

Table 2. The variables d_R, d_I, g_R, g_I (doubly deflected cracks) as a function of α

α	d_R	d_I	g_R	g_I
−0.9	0.0513	−0.5128	1.776	0.0333
−0.8	0.0901	−0.5089	1.791	0.0614
−0.7	0.1358	−0.4877	1.798	0.0857
−0.6	0.1796	−0.4624	1.808	0.1078
−0.5	0.2233	−0.4361	1.814	0.1280
−0.4	0.2629	−0.4104	1.824	0.1465
−0.3	0.3005	−0.3860	1.830	0.1639
−0.2	0.3351	−0.3627	1.833	0.1803
−0.1	0.3677	−0.3411	1.839	0.1962
0.0	0.3973	−0.3208	1.845	0.2117
0.1	0.4250	−0.3019	1.847	0.2251
0.2	0.4304	−0.2841	1.853	0.2397
0.3	0.4736	−0.2675	1.854	0.2517
0.4	0.4951	−0.2523	1.856	0.2655
0.5	0.5147	−0.2379	1.865	0.2767
0.6	0.5330	−0.2245	1.864	0.2879
0.7	0.5499	−0.2123	1.873	0.2996
0.8	0.5649	−0.2004	1.870	0.3107
0.9	0.5790	−0.1886	1.871	0.3196

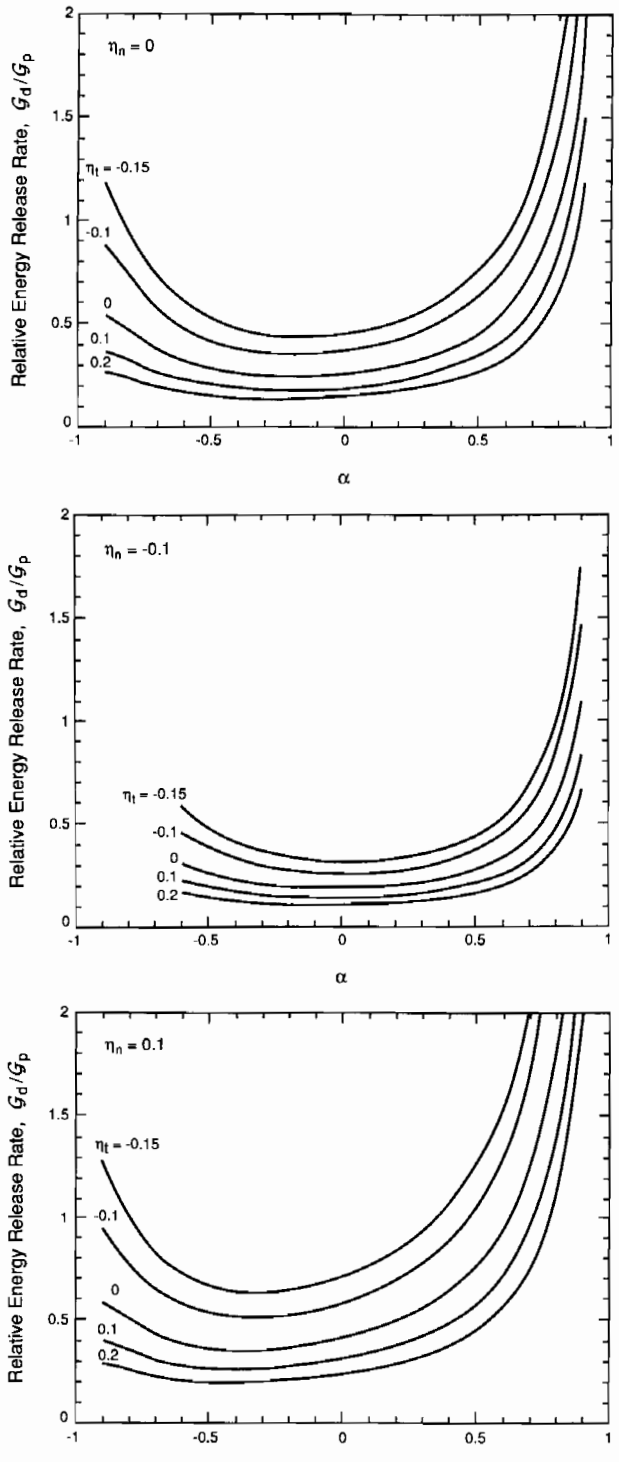

Fig. 3. Energy release rate ratio as a function of α for various values of the residual stress parameter η_t. $\mathcal{G}_d$ is the energy release rate of the singly deflected crack. (a) $\eta_n = 0$; (b) $\eta_n = -0.1$; (c) $\eta_n = 0.1$.

and (b) the corrected results for $\mathcal{G}_d/\mathcal{G}_p$ and Ψ as functions of α for the case of $\eta_t = \eta_n = 0$. These corrections agree with results computed independently by Martinez and Gupta (1993) and Tullock *et al.* (1994).

The transition toughness ratio separating interface debonding and penetration is given by

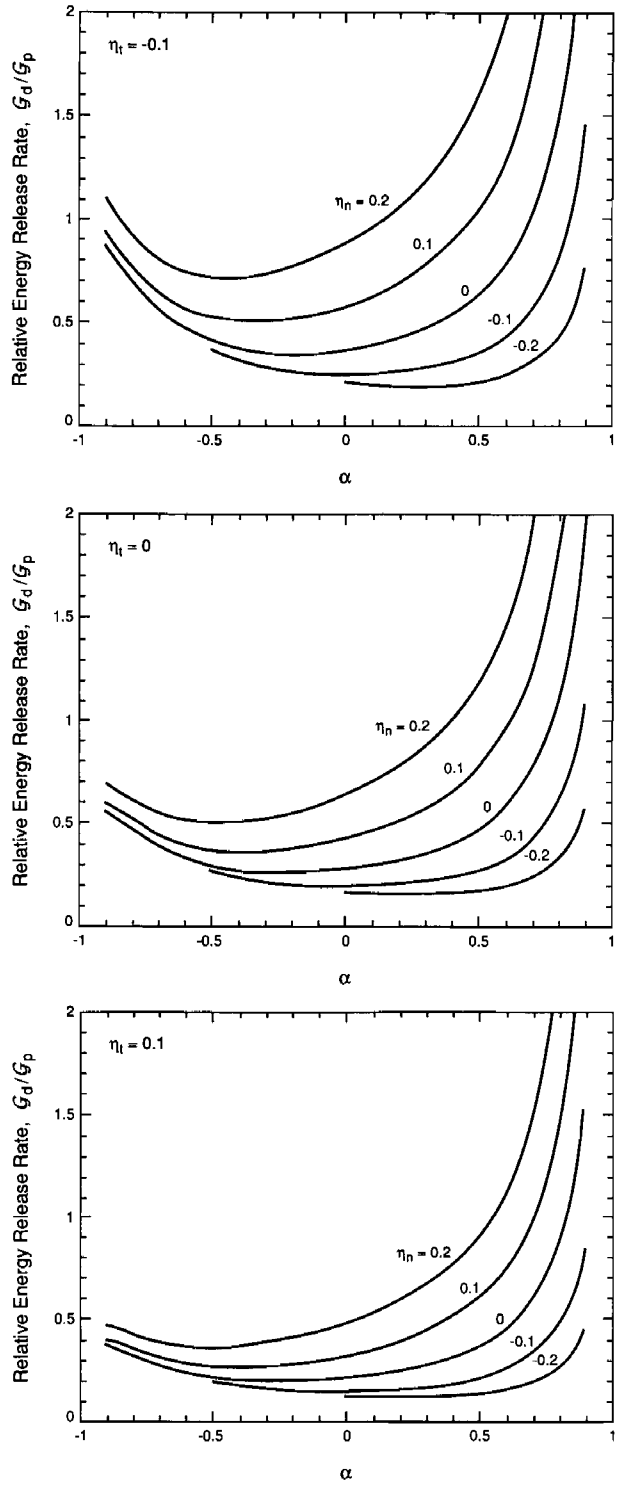

Fig. 4. Energy release rate ratio as a function of α for various values of the residual stress parameter η_n. $\mathcal{G}_d$ is the energy release rate of the singly deflected crack. (a) $\eta_t = -0.1$; (b) $\eta_t = 0$; (c) $\eta_t = 0.1$.

$$\left(\frac{\Gamma_i}{\Gamma_s}\right)_{\text{Trans}} = \frac{\mathcal{G}_d}{\mathcal{G}_p} \tag{17}$$

where, as previously defined, Γ_s is the mode I toughness of material 1 and Γ_i is the interface toughness associated with the mixed-mode loading of the kinked crack tip. Consequently,

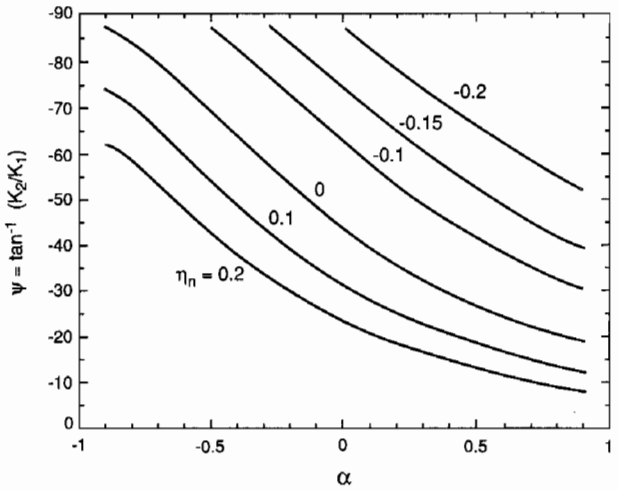

Fig. 5. The trends in phase angle Ψ of the singly deflected interface crack with α for various values of the residual stress parameter η_n.

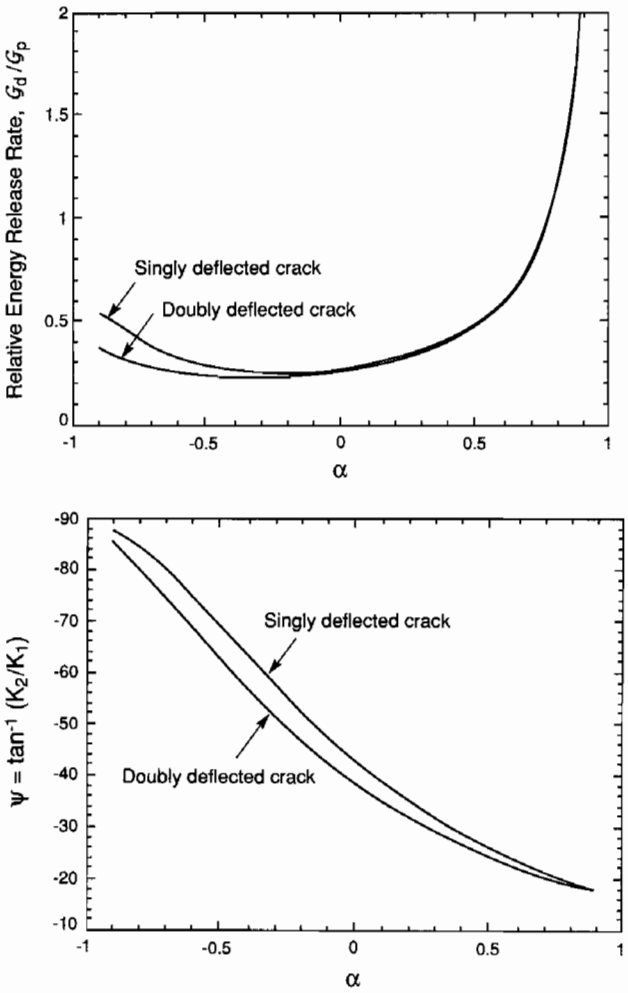

Fig. 6. (a) Ratio of energy release rate of deflected cracks to penetrating crack at the same amount of crack advance a. The result for the doubly deflected crack corrects an earlier plot given in He and Hutchinson (1989b). (b) The trends in phase angle Ψ of the deflected cracks.

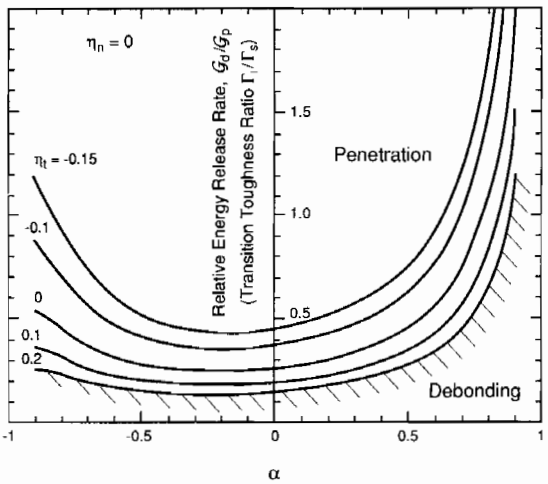

Fig. 7. Energy release rate ratio as a function of α for various values of the residual stress parameter η_n.

the plots of energy release rate ratio may also be used to define the debonding and penetration regimes, as illustrated in Fig. 7. The curves would be used as follows. The qualities η_t and η_n would be evaluated having knowledge of the residual stresses and the size of the flaws at the interface, a_d, and in the next layer, a_p. These quantities also require knowledge of k_I. When there is no elastic mismatch, k_I is just the conventional mode I stress intensity factor K_I for the main crack and $\lambda = 1/2$. If the elastic mismatch is not too large, one can approximate $k_I a^{-\lambda}$ in eqn (1) by $K_I a^{-1/2}$ where K_I is the conventional factor for the homogeneous problem. However, when the mismatch is large and if an *accurate* estimate of η is required, then the solution for k_I for the main crack problem must be used. An example in the literature is in Ballarini and Luo (1991). Then, with independent information about the elastic mismatch, α, the figure dictates whether the interface is located in either the penetration or debonding regime.

When the interface is in residual tension, two factors dictate that, once debonding is initiated, the debond crack becomes unstable: (i) η_n increases as the debond crack length, a_d, increases; and (ii) as η_n increases, the phase angle Ψ decreases, causing $\Gamma_i(\Psi)$ to decrease, through the effect of phase angle on the interface fracture energy (Hutchinson, 1990).

Conversely, compressive residual stresses ($\eta_t < 0$ or $\eta_n < 0$) lead to stable crack extension following either debonding or penetration, because η becomes more negative as the cracks extend.

3. IMPLICATIONS

The marked shifts in the debond–penetration boundaries with both normal and in-plane residual stresses, reflected in η_n and η_t, has a major implication for the behavior of cracks in layered materials and in fiber composites. In *layered materials*, η_n is usually zero and the incidence of interface debonding is dominated by η_t. The key implications can be drawn directly from Fig. 7. Interface debonding effects that can lead to an enhanced fracture resistance, compared with the constituent materials are encouraged by interposing thin layers that have both a high elastic modulus (large positive α) and a low thermal expansion coefficient that results in negative η_t. A diagram that plots debonding–penetration loci (Fig. 8) as functions of elastic mismatch and residual stress for specific fracture energy ratios, Γ_i/Γ_s is of particular utility for identifying conditions that lead to debonding. It is notable that debonding can even occur when the interface has the same fracture energy as the reinforcing material ($\Gamma_i \approx \Gamma_s$) when α and η_t are sufficiently large.

In fiber composites, the problem is more complex because η_n and η_t are connected, arising from the thermal expansion mismatch between the fiber and the matrix (Budiansky *et al.*, 1986). An expression for the ratio of η_n to η_t when $a_p \approx a_d$ demonstrates this

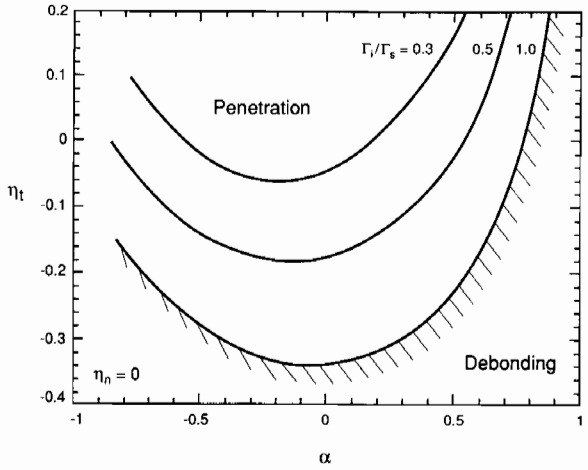

Fig. 8. Debond loci for given Γ_i/Γ_s, plotted in η_t, α space, as needed to identify the interface fracture energies that cause debonding in layered structures.

connection. This formula is obtained from Budiansky *et al.* (1986) under the assumptions that the thermal expansion mismatch is isotropic and $\nu_f = \nu_m$,

$$\eta_t/\eta_n \equiv \sigma_t/\sigma_n = [(1+f)(1+\alpha)+(1-f)(1-\alpha)]/[f(1+\alpha)+(1-f)(1-\alpha)] \tag{18}$$

where f is the fiber volume fraction. Consequently, to address debonding for this case, it is more convenient to express the results in terms of a single misfit stress parameter, defined as:

$$\eta_q = E_m \Omega a_d^i / k_1 \tag{19}$$

where Ω is the misfit strain. Then, the ratio $\mathcal{G}_d/\mathcal{G}_p$ can be plotted as a function of f for various thermal expansion misfits as measured by η_q, assuming eqn (18) holds [Fig. 9(a)]. It is apparent that, while η_q can have a strong influence on debonding at small f (especially when α is large and positive), debonding is only weakly dependent on thermal expansion mismatch at fiber volume fraction typically used in composites ($f \gtrsim 0.3$) and at more modest elastic mismatches [Fig. 9(b)].

4. CONCLUDING REMARKS

Residual stresses governed by thermal expansion misfit are shown to have substantial importance on the competition between interface debonding and crack penetration when the interfaces are planar, as in layered material, in thin film structures, etc. However, in fiber composites, because of the coupling between axial and radial residual stress, the effects of misfit on fiber debonding at matrix cracks will generally be minimal, at fiber volume fractions used in practice.

The effect of residual stresses in layered materials may be used to advantage for designing interfaces that impart damage tolerant behavior, as found in certain naturally occurring materials, such as shells.

Acknowledgements—This work was supported by the Defense Advanced Research Projects Agency through the University Research Initiative under Office of Naval Research Contract No. N-00014-86-K-0753. The authors with to express their appreciation to Richard Carr of Harvard University who carried out some of the calculations for the doubly deflected crack. We also wish to thank V.J. Gupta, A. Graham and P.S. Steif for independently calling our attention to the error in the solution to the doubly deflected crack problem in He and Hutchinson (1989b). Helpful suggestions by reviewers are gratefully acknowledged.

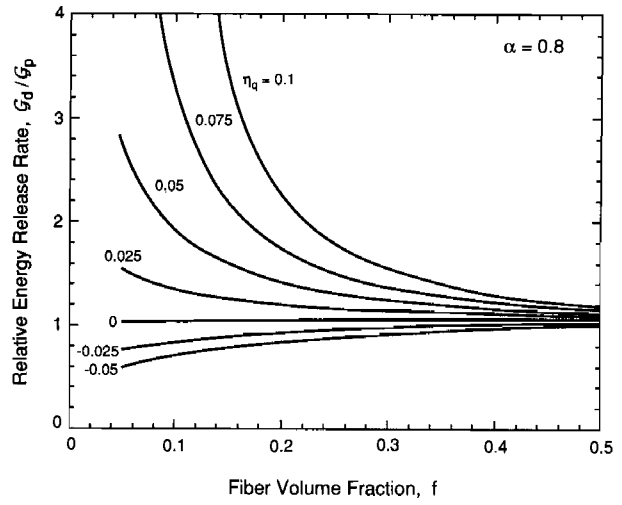

(a)

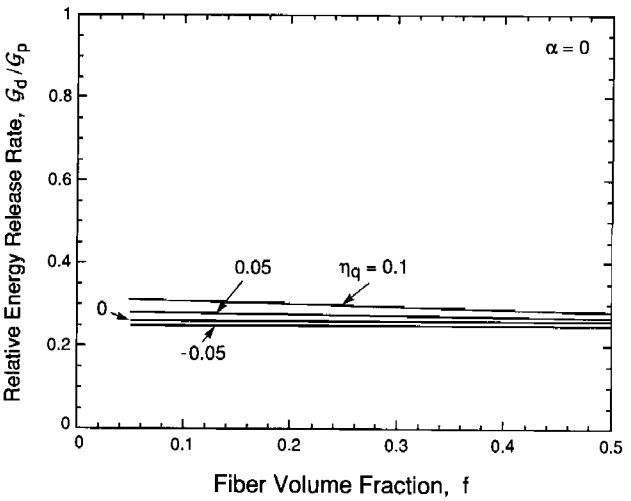

(b)

Fig. 9. Energy release rate ratio for fiber composites as a function of the fiber volume fraction, for various values of the residual stress parameter η_q. (a) $\alpha = 0.8$; (b) $\alpha = 0$.

REFERENCES

Ballarini, R. and Luo, H. A. (1991). Green's functions for dislocations in bonded strips and related crack problems. *Int. J. Fracture* **50,** 239–262.

Budiansky, B., Hutchinson, J. W. and Evans, A. G. (1986). Matrix fracture in fiber-reinforced ceramics. *J. Mech. Phys. Solids* **34** (2), 167–189.

Evans, A. G., Dalgleish, B. J., He, M. Y. and Hutchinson, J. W. (1989a). On crack path selection and the interface fracture energy in bimaterial systems. *Acta Metall.* **37** (12), 3249–3254.

Evans, A. G., He, M. Y. and Hutchinson, J. W. (1989b). Interface debonding and fiber cracking in brittle matrix composites. *J. Am. Ceram. Soc.* **72** (12), 2300–2303.

He, M. Y. and Hutchinson, J. W. (1989a). Kinking of a crack out of an interface. *J. Appl. Mech.* **56** (2), 270–278.

He, M. Y. and Hutchinson, J. W. (1989b). Crack deflection at an interface between dissimilar elastic materials. *Int. J. Solids Structures* **25** (9), 1053–1067.

Hutchinson, J. W. (1990). Mixed mode fracture mechanics of interfaces. In *Metal/Ceramic Interfaces* (Edited by M. Rühle and A. G. Evans). Pergamon Press, Elmsford, NY.

Martinez, D. and Gupta, V. (1993). Energy criterion for crack deflection at an interface between two orthotropic media. II. Results and experimental verification. *J. Mech. Phys. Solids.* **42** (8) (MPS 81).

Rice, J. R. (1988). Elastic fracture mechanics concepts for interfacial cracks. *J. Appl. Mech.* **55** (1), 98–103.

Tada, H., Paris, P. C. and Irwin, G. R. (1985). *The Stress Analysis of Cracks Handbook*, 2nd edition. Paris Productions Incorporated, Paris.

Tullock, D. L., Reimanis, I. E., Graham, A. L. and Petrovic, J. J. (1994). Deflection and penetration of cracks at an interface between two dissimilar materials. *Acta Metall. Mater.* **42,** 3245–3252.

Zak, A. R. and William, M. L. (1963). Crack point singularities at a bimaterial interface. *J. Appl. Mech.* **30** (1), 142–143.

APPENDIX: FINITE ELEMENT METHOD

The model employed in the finite element calculation is a circular region $r \leqslant R$. In order to obtain the asymptotic solution, R should be much larger than the length of the branch crack (a_p or a_d). A general purpose finite element code, ABAQUS, is used, with very fine meshes. For example, the mesh for the singly deflected crack problem [Fig. 1(c)] contains 1480 eight-node isoparametric elements and 4876 nodes. Figure A1(a) shows the central core of the mesh in the vicinity of the deflected crack. Outside this core, the mesh has 35 layers of elements in the radial direction (from the core to the external boundary) and 32 elements in the circumferential direction. Figure A1(b) shows the 19 layers of elements next to the external boundary. Due to the symmetry, only a semi-circular region is needed for the penetrated or the doubly deflected crack problems.

An indication of the convergence of the asymptotic value of h, as dependent on the ratio R/a_p, can be seen in Table A1 for the penetrated crack problem. For the homogeneous material ($\alpha = 0$), the results from $R/a_p = 500$

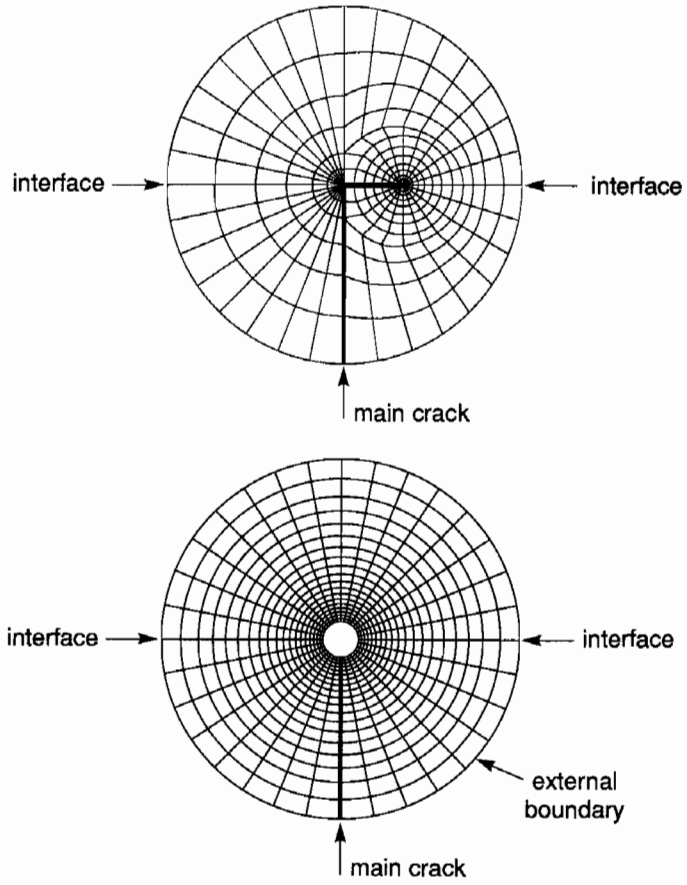

Fig. A1. (a) The central core of the finite element mesh in the vicinity of the deflected crack. (b) The finite element mesh for the region next to the external boundary.

Table A1. The variable h

R/a_p		100	200	300	500	1000	2000	4000
h	$\alpha = 0$	1.626	1.611	1.606	1.602	1.599	1.597	
	$\alpha = 0.5$	1.771	1.763	1.760	1.758	1.757	1.756	1.754
	$\alpha = -0.9$	1.400	1.362	1.346	1.330	1.314	1.302	1.295

indicate that h compares with the analytical results of Tada *et al.* (1985) ($h = \sqrt{8/\pi} = 1.5958$) to three significant figures. For $\alpha = 0.5$, the difference between the calculation with ($R/a_p = 200$) and that with ($R/a_p = 500$) is less than 0.5%. For $\alpha = -0.9$, the convergence is slower; however, the difference between the calculation with ($R/a_p = 1000$) and that with ($R/a_p = 2000$) is less than 1%. Convergence checks for the singly deflected crack reveal the same general tendency. The results shown in Table A1 indicate the ratio $R/a_p(a_d) = 1000$ is large enough to obtain the asymptotic solutions. All of the results shown in this paper were obtained with R/a_p or $R/a_d = 1000$.